Headline Indicators for Global Climate Monitoring

Blair Trewin, Anny Cazenave, Stephen Howell, Matthias Huss, Kirsten Isensee, Matthew Palmer, Oksana Tarasova, Alex Vermeulen

Headline indicators for global climate monitoring

Blair Trewin[1], Anny Cazenave[2], Stephen Howell[3], Matthias Huss[4,9], Kirsten Isensee[5], Matthew D. Palmer[6], Oksana Tarasova[7] and Alex Vermeulen[8].

1. Australian Bureau of Meteorology, Melbourne.
2. LEGOS, Observatoire Midi-Pyrenees, Toulouse, France.
3. Climate Research Division, Environment and Climate Change Canada, Toronto, Canada.
4. Laboratory of Hydraulics, Hydrology and Glaciology (VAW), ETH Zuerich, Zuerich, Switzerland
5. Intergovernmental Oceanographic Commission, UNESCO, Paris, France.
6. Met Office Hadley Centre, Exeter, United Kingdom.
7. World Meteorological Organization, Geneva, Switzerland.
8. Lund University, Lund, Sweden.
9. Swiss Federal Institute for Forest, Snow and Landscape Research (WSL), Birmensdorf, Switzerland.

Corresponding author: Blair Trewin, Australian Bureau of Meteorology, GPO Box 1289, Melbourne VIC 3001, Australia. E-mail: blair.trewin@bom.gov.au.

Abstract

The World Meteorological Organization has developed a set of headline indicators for global climate monitoring. These seven indicators are a subset of the existing set of Essential Climate Variables (ECVs) established by the Global Climate Observing System and are

Early Online Release: This preliminary version has been accepted for publication in *Bulletin of the American Meteorological Society*, may be fully cited, and has been assigned DOI 10.1175/BAMS-D-19-0196.1. The final typeset copyedited article will replace the EOR at the above DOI when it is published.

intended to provide the most essential parameters representing the state of the climate system. These indicators include global mean surface temperature, global ocean heat content, state of ocean acidification, glacier mass balance, Arctic and Antarctic sea ice extent, global CO_2 mole fraction , and global mean sea level. This paper describes how well each of these indicators are currently monitored, including the number, and quality of the underlying data sets; the health of those data sets; observation systems used to estimate each indicator; the timeliness of information; and how well recent values can be linked to pre-industrial conditions. These aspects vary widely between indicators. Whilst global mean surface temperature is available in close to real time and changes from pre-industrial levels can be determined with relatively low uncertainty, this is not the case for many other indicators. Some indicators (e.g., sea ice extent) are largely dependent on satellite data only available in the last 40 years, while some (e.g., ocean acidification) have limited underlying observational bases, and others (e.g. glacial mass balance) with data only available a year or more in arrears.

Capsule

A set of headline global climate indicators has been developed to support assessments of the state of the global climate.

Introduction

A wide range of variables is used to monitor the state of the global climate. This monitoring includes reporting on annual timescales, such as through the World Meteorological Organisation (WMO)'s State of the Climate series (e.g., WMO, 2019) and the State of the Climate reports published through the Bulletin of the American Meteorological Society (e.g.,

Accepted for publication in *Bulletin of the American Meteorological Society.* DOI 10.1175/BAMS-D-19-0196.1.

Blunden et al., 2018), as well through the systematic Assessment Reports of the Intergovernmental Panel on Climate Change (IPCC) (IPCC, 2013, 2019a, 2019b).

Key indicators play an important role in many forms of global monitoring. They are quantified, objective, based on data provided by virtually all countries, and they are used to demonstrate change in the climate system over time. The Parties to the United Nations Framework Convention on Climate Change (UNFCCC) are also likely to include indicators in the "global stocktake", an assessment made every five years to measure progress under article 14 of the Paris Agreement (United Nations, 2015a). The ongoing negotiations on how to structure this process and on what information to include in the stocktake are due for finalisation before the first stocktaking exercise takes place in 2023.

The main framework for determining key variables representing the state of the climate system has hitherto been the Global Climate Observing System (GCOS) set of Essential Climate Variables (ECVs) (Bojinski et al., 2014; Table 1), a concept which dates from the early 2000s. This set consists of 54 different variables (16 atmospheric, 19 ocean and 19 terrestrial), some of which have multiple indicators associated with them, and includes variables which are measured using conventional surface and upper-air meteorological observations, as well as many which are primarily measured using means such as remote sensing platforms or ocean-based platforms. An assessment of how well ECVs are monitored forms the core of regular assessments of the status of the global climate observing system (e.g. WMO, 2015). Some variables, such as surface temperature, are supported by the comprehensive global observing networks, a long history of observations, and well-established mechanisms for international data exchange and archiving, whilst for

Accepted for publication in *Bulletin of the American Meteorological Society.* DOI 10.1175/BAMS-D-19-0196.1.

some other variables (particularly ocean and terrestrial variables), the amount of information available is much more limited.

The ECVs provide the basis for a comprehensive assessment of the state of the global climate system, but form a complex picture, particularly for communicating with policymakers and non-specialists. Frequently in public discourse, assessments like the WMO State of the Global Climate statement and similar reports are communicated via a single indicator, global mean surface temperature. To address this, WMO, in conjunction with the World Climate Research Program (WCRP) and GCOS developed a new set of headline climate indicators. The primary objective (Williams and Eggleston, 2017) is to provide a range of indicators which gives a more comprehensive picture of the overall state of the global climate system than surface temperature alone. These indicators should be scientifically robust and cover the atmosphere, ocean and cryosphere, whilst still being sufficiently simple and few in number (ideally between five and ten) to be suitable for widespread public communication. The indicators are targeted particularly at high-level policy events such as the activities of the UNFCCC, but we expect that they will also be valuable for broader reporting of the state of the global climate.

The desired characteristics (Williams and Eggleston, 2017) for the headline climate indicators were as follows:

***Relevance**:* each headline indicator should be a clear, understandable indicator of the state of the climate system, with broad relevance for a range of audiences, whose value can be

Accepted for publication in *Bulletin of the American Meteorological Society.* DOI 10.1175/BAMS-D-19-0196.1.

expressed as a single number. Some such global indicators may also have value at the national and regional levels.

Representativeness: the indicators as a package should provide a representative picture of a broad range of changes to the Earth system related to climate change.

Traceability: each indicator should be calculated using an internationally agreed upon (and published) method and accessible and verifiable data.

Timeliness: each indicator should be calculated regularly (at least annually), with the minimum possible time between the end of the period and publication of the data.

Data adequacy**:** the available data needed for the indicator calculation must be sufficiently robust, reliable and valid.

Seven headline indicators (Table 2), each of which draws on one or more ECVs, were finalised by the WMO's Commission for Climatology at its 2018 meeting (WMO, 2018a), following earlier discussions at meetings of WMO and GCOS in February (WMO 2017a, GCOS 2017) and October 2017. These took the above criteria into account whilst providing the broadest possible picture of the state of the climate system. These were first formally reported by WMO (for the five indicators which at that time had available data for 2017) in the 2017 State of the Climate report (WMO, 2018c).

The purpose of this paper is to assess how well each of the seven indicators chosen by WMO is supported by the underlying observation and computational methodology, and, for some of the less completely observed indicators, what is required to improve their monitoring into the future to allow the criteria above to be fully met. The indicators are intended for use of global level; whilst many of them will also be applicable at smaller

spatial scales, other indicators will also be required for local climate assessment. There are numerous other potential indicators, especially for atmospheric variables, which broadly meet the criteria above (Table S2) but have not been included in the interests of keeping the total number of indicators manageably small.

The way in which these indicators are conventionally expressed varies from indicator to indicator. For example, mean global mole fraction of CO_2 is most often expressed as absolute value, glacial mass balance as a year-on-year change, and temperature as an anomaly or departure from the average of a given baseline period. The choice of baseline period depends on the indicator and the availability of data. The most commonly used baseline period is 1981-2010 (WMO, 2017b), especially for indicators which draw on satellite data sets which begin in the 1970s, whilst another example of a baseline period, used particularly for temperature, is 1850-1900, used as an approximation to pre-industrial conditions by IPCC (Allen et al., 2018). The choice of baseline shifts absolute values but has little or no impact on the estimation of changes or trends.

The headline indicators

Temperature

Global mean surface temperature (GMST) is arguably the best-known metric used in monitoring the state of the climate. Conventionally, it is defined using a combination of air temperature at screen level (2 m) over land, and sea surface temperature (SST) in ocean

Accepted for publication in *Bulletin of the American Meteorological Society.* DOI 10.1175/BAMS-D-19-0196.1.

areas. It is conventionally expressed as an anomaly from a baseline period, although the baseline period used differs between different data sets.

A number of global data sets are maintained by various institutions (Table S1). These combine historical data drawn from a range of sources with data collected through national meteorological services and transmitted in near-real time through the WMO's Global Telecommunications System, particularly the monthly CLIMAT reports from land stations, while the International Comprehensive Ocean-Atmosphere Data Set (ICOADS; Freeman et al., 2017) is a major data source for SST data. More recently, reanalyses have also been used for the assessment of global temperatures, using the (not strictly equivalent) definition of air temperature over the oceans rather than SST. As updating is drawn from sources which normally report within a few days of the end of each month, these GMST analyses are normally available for each month within 1-2 weeks of the end of the month for reanalyses, and 2-4 weeks for "conventional" data sets.

All of the data sets listed in Table S1 have been the subject of extensive assessment of their quality and homogeneity. The largest differences between them, particularly in more recent years, relate to the way in which they do (or do not) interpolate over data-sparse areas such as the polar regions, with approaches ranging from that of HadCRUT4 (which treats 5° x 5° grid boxes with no data as missing) to the reanalyses, whose data are spatially complete (Figure 1), and Cowtan and Way (2014), who use satellite data to extend surface analyses to polar regions. As the Arctic is warming much faster than the rest of the globe (Davy et al., 2018), the more spatially complete data sets show stronger recent warming trends than those with limited Arctic representation (Simmons et al., 2017). The treatment of systematic

Accepted for publication in *Bulletin of the American Meteorological Society.* DOI 10.1175/BAMS-D-19-0196.1.

biases associated with changes in the way that SST are measured is also significant (e.g. Kennedy et al., 2019).

Current values of GMST can be linked to the pre-industrial period with a modest level of uncertainty (Hawkins et al., 2017). Although the pre-industrial period was not formally defined in the Paris Agreement, IPCC has adopted 1850-1900 as a working definition of a pre-industrial-equivalent baseline. Of the data sets in Table S1, only HadCRUT4 and BEST cover the full 1850-1900 period, with other conventional data sets starting in 1880, but methods have been developed (Allen et al., 2018) to connect those data sets (and the reanalyses) to a 1850-1900 baseline. Uncertainties in instrumental GMST in the 1850-1900 period, particularly the early part of it, are larger than for more recent data, because of sparse data coverage (especially for Southern Hemisphere land areas), and potential residual uncertainties associated with non-standardisation of instrument shelters and SST measurement methods (Morice et al., 2012).

Ocean heat content

A defining characteristic of the global ocean is a large capacity to store and transport heat. The upper few metres of the global ocean have the same heat capacity as the entire atmosphere (Gill, 1982). It is estimated that over 90% of the radiative imbalance associated with anthropogenic climate change is absorbed by the oceans, with the remaining 10% going into heating of the land surface, atmosphere and cryosphere (von Schuckmann et al., 2016). The ocean's dominant role in the planetary energy budget arises at annual timescales (Palmer and McNeall, 2014) and makes ocean heat content (OHC) change a primary

observational metric of global warming because it provides a strong constraint on the magnitude of Earth's energy imbalance (von Schuckmann et al., 2016; Palmer, 2017). In addition, OHC is less subject to interannual to decadal variability than global mean surface temperature (Palmer and McNeall, 2014; Wijffels et al., 2016).

The primary means of estimating OHC change is through analysis of historical subsurface temperature profiles. The methods used are broadly similar to those applied to global surface temperature; a number of profiles in a given time "window" are spatially interpolated to estimate the global average, relative to a reference period. As with surface temperature, inter-platform biases are assessed and corrected for, e.g. those associated with expendable bathythermograph (XBT) instruments (Abraham et al., 2013; Cheng et al., 2016). A number of indirect methods for estimating OHC change are also available, such as satellite-based estimates of ocean thermal expansion and ocean data assimilation products that combine the available observations with a dynamical ocean model (Meyssignac et al, 2019).

A key challenge for estimating OHC change is the highly heterogeneous and depth-limited historical ocean sampling (Abraham et al, 2013; Palmer, 2017). Estimates of annual OHC change that extend back to the mid-20th century (Figure 2) are typically limited to the 0-700 m depth layer and have particularly large sampling uncertainties before the mid-1960s (Lyman and Johnson, 2008; Palmer and Brohan, 2011; Abraham et al, 2013; Cheng et al, 2017). Since the mid-2000s, the Argo array of autonomous profiling floats has provided near-global coverage of the upper 2000 m of the ice-free ocean and a dramatic

improvement in our ability to monitor OHC change (Riser et al, 2016), with greater consistency between data products.

Estimates of sub-2000 m OHC change rely on a sparse network of full-depth hydrographic sections from scientific research vessels that permit estimation of decadal trends in OHC from about the 1990s onwards (Purkey and Johnson, 2010; Desbruyères et al., 2016). However, combined with Argo observations, this information allows us to estimate the global OHC change over the full-depth from the mid-2000s and also characterise the spatial time-evolution of the warming (Desbruyères et al., 2017). While the observational basis is less robust, some recent estimates of full-depth OHC change extend back to 1960 (Cheng et al., 2017).

Time series of global OHC anomaly from a number of semi-operational products are presented routinely as part of the annual BAMS State of the Climate report (e.g. Blunden et al., 2018). The data include annual time series for the 0-700 m and 700-2000 m layers, and an estimate of the long-term trend for ocean below 2000 m. The data products are based on various interpolation methods and may also vary in their approach to XBT bias correction (Boyer et al. 2016). While statistically based estimates remain prevalent for monitoring OHC change, ocean data assimilation products ("ocean reanalyses") are also increasingly being used (e.g. Palmer et al, 2017). An ensemble of four ocean reanalyses is used to provide annual time series of global OHC change for the 0-700 m and 0-2000 m layers from 1993 onwards as part of the Copernicus Marine Service Ocean State Report (von Schuckmann et al., 2018).

Linking the current OHC state robustly to the pre-industrial climate is extremely challenging, owing to the lack of subsurface temperature observations during the period 1850-1900. The primary source of data we have in this regard is the *HMS Challenger* Expedition, which took place between 1872 and 1876. Although the *Challenger* subsurface temperature observations were global in scope, they were taken along a small number of ship tracks, mostly confined to 40° N to 40° S in the Atlantic and Pacific oceans (Roemmich et al., 2012). These data have been used to assess the change in OHC for 0-700 m between the 1872-1876 and 2004-2010 (Roemmich et al., 2012), albeit with large uncertainties. Further insights into the OHC state during preindustrial times may be afforded by more novel approaches, such as the Green's Function method used by Zanna et al. (2019. This method uses an estimate of ocean circulation to propagate observed surface temperature anomalies into the ocean interior and therefore provide an estimate of change in ocean heat content since 1871.

Since the mid-2000s, Argo provides the vast majority of subsurface temperature profiles used for in situ-based estimates of OHC change. While these data are provided in near real-time, the highest quality "delayed-mode" data (Wong et al, 2018) may have a 1-2- year time lag associated with them. Public release of research cruise data is often the responsibility of the cruise principal investigator and can result in delays of several years.

Sea level

Accepted for publication in *Bulletin of the American Meteorological Society.* DOI 10.1175/BAMS-D-19-0196.1.

The global mean sea level (GMSL) is recognized as a leading indicator of global climate change because it reflects changes occurring in multiple different components of the climate system (ocean, atmosphere, cryosphere and hydrosphere) and their mutual interactions.

Historically, sea level has been measured by tide gauges located along continental coastlines and islands but the coverage of long, good quality tide gauges is heterogeneous and biased towards the northern hemisphere for most of the 20th century. This tide-gauge-based sea level record, despite its limited geographical coverage, provides a fundamental historical reference for long-term sea level studies. Since the early 1990s, sea level is routinely monitored with near-full global coverage by high precision satellite altimetry (Figure 3) that provides 'absolute' sea level data in a geocentric reference frame (unlike tide gauges that also sense vertical land motions). This allows the routine estimation of GMSL as a climate indicator from 1993 onwards.

Since the launch of the TOPEX/Poseidon mission in 1992, there is now a 27-year long sea level record from which the global mean sea level rise can be inferred as well as regional trends (Cazenave et al., 2019). The satellite altimetry constellation includes the so called 'reference' missions (TOPEX and Jason-1,2 &3, covering the 66°N/S latitude domain, and providing the most accurate long-term stability of sea level measurements at global and regional scales). There are also complementary satellites covering part of the Arctic ocean, up to 82°N latitude (ERS-1&2, Envisat, Saral/AltiKa, Sentinel-3A&B). Different groups worldwide provide altimetry-based GMSL time series, which can be updated with less than one month's delay using Jason-3 data, as well as gridded data sets. Although different

Accepted for publication in *Bulletin of the American Meteorological Society.* DOI 10.1175/BAMS-D-19-0196.1.

processing approaches are implemented by these groups, the quality of the different GMSL time series is similar. Long-term trends agree well to within 6% of the signal, approximately 0.2 mm/yr in terms of trend, well within the GMSL trend uncertainty range estimated to around 0.3 mm/yr from tide gauge comparison and error assessments of all sources of uncertainties affecting the altimetry system.

This 27-year long record indicates that the global mean sea level continues to rise at a mean rate of 3.2 +/- 0.3 mm/yr, with some evidence of acceleration. The acceleration (about 0.1 mm/yr^2) results of increased ocean thermal expansion (due to ocean warming) and ice mass loss from glaciers, Greenland and Antarctica (WCRP, 2018, Nerem et al., 2018).

Regular assessments of the global mean sea level budget have been recently initiated for the altimetry era, a period for which different observing systems are available (e.g., Argo profiling floats for the ocean thermal expansion component and GRACE space gravimetry for the mass components). These budget studies that indicate that in terms of global mean, the sea level budget is closed within quoted uncertainties (e.g., WCRP, 2018, Horwath et al., 2020) are important for many reasons. Quasi closure of the sea level budget indicates that no systematic errors affect the different observing system and that there is no important missing contribution (e.g., from the deep ocean not sampled yet by Argo). They allow improved process understanding and detection of temporal change (e.g., acceleration or abrupt change) in the components, and may be useful for validating the climate simulations used for projections (although the current record is still short for the latter application). Finally, the altimetry-based global mean sea level corrected for the mass components (e.g., the GRACE-based ocean mass contribution) is a proxy of the total ocean heat content. It provides thus another approach to monitor the global mean OHC, independently from in

situ ocean temperature measurements, with applications for estimating the Earth's energy imbalance (von Schuckmann et al., 2016).

While the GMSL remains a major climate indicator, for coastal communities, what matters is 'relative' coastal sea level change ('relative' means with respect to the Earth crust), i.e. the sum of the GMSL plus superimposed regional variability plus small- scale coastal processes. The latter include small-scale shelf currents, changes in wind and waves, and fresh water input from river estuaries (that modifies the density structure of sea water). Moreover, at the coast, vertical land motions due to natural or anthropogenic factors (such as ground subsidence from hydrocarbon or water extraction, or sediment compaction in river deltas) will superimpose on the global mean and regional sea level components. Such vertical land motions amplify the climate-related sea level rise in many places, although in others they offset it.

Sea ice extent

Sea ice extent is the most widely used climate indicator to assess long term changes in Arctic and Antarctic sea ice. Sea ice extent is defined as the area covered by an areal ice concentration greater than 15%. It is typically derived from passive microwave satellite measurements that are available in close to real time and provide a consistent observational record that now spans more than 40 years. There are several different sea ice datasets that make use of passive microwave satellite measurements, and different retrieval algorithms. Therefore, the uncertainty varies depending on the dataset. Resolving the position of ice edge or marginal ice zone, thin ice and melt ponds forming on the surface of the sea ice are the primary sources of uncertainty (Ivanova et al., 2015; Comiso et al.,

2017). To that end, the differences in sea ice extent between datasets can range from $0.5x10^6$ km^2 to $1x10^6$ km^2 (Meier and Stewart, 2019). Further, construction of more than 40 years sea ice extent record requires combining sensors of shorter operational lifetimes together; therefore, uncertainty can vary temporally depending on the quality of sensor calibration (Eisenman et al., 2014). Despite these differences, the long-term datasets of passive microwave satellite derived measurements of sea ice extent still provide the most robust and consistent indictor of long-term change (Comiso et al., 2017).

Figure 4 shows the time series of sea ice extent anomalies for the Arctic in March (winter maximum) and September (summer minimum) as well as for the Antarctic in September (winter maximum) and February (summer minimum) for two of the most common, widely used and available in close to real time sea ice extent datasets, the Sea Ice Index Version 3 (Fetterer et al., 2017) and Satellite Application Facility on Ocean and Sea Ice (OSI-SAF) Version 2 (Lavergne et al., 2019). Note the inter-annual variability is similar between these two products. In the Arctic, the summer minimum sea ice extent has declined at a rate of around 12.5% per decade and winter maximum sea ice extent has declined at a rate of around 2.7% per decade over the 1979-2019 period. Reductions are particularly prominent in the Beaufort and Chukchi Seas during the summer and in the Barents and Bering Seas during the winter. Overall, the downward trend in the Arctic's September sea ice extent is perhaps one of the most visually striking indicators of climate change. In the Antarctic, there has been considerably more interannual variability in both summer and winter sea ice extents in addition to a weak increasing trend up until 2014 that contrasts the strong negative trend in the Arctic. However, this positive Antarctic trend has been found to have

reversed in 2014 with the recent decreasing sea ice extent rates greater than observed in the Arctic (Parkinson, 2019).

There is evidence to suggest that the recent decline in Arctic September sea ice extent observed over the post-1979 satellite record is unprecedented compared to historical reconstructions for the pre-1979 period (Walsh et al., 2017) and paleoclimate proxy data (e.g. Kinnard et al., 2011). Pre-1979 observations for the Antarcticpoint to a decrease in February sea ice extent (Abram et al., 2013; Gallaher et al., 2014) but there is considerable uncertainty in these observations and therefore it is difficult to link these with the more consistent post-1979 satellite observations (Hobbs et al., 2016).

A concern with the 40+ year passive microwave sea ice extent record is that the remaining satellites in orbit are well beyond their operational lifetime (Witze, 2017). However, the European Organisation for the Exploitation of Meteorological Satellites (EUMETSAT) Polar System – Second Generation (EPS-SG) which is expected to launch in 2023 will contain sensors to facilitate the continuation of the 40+ year passive microwave sea ice extent record. In addition, there is the Copernicus Imaging Microwave Radiometer (CIMR) mission that is currently a candidate mission (high priority) within the European Copernicus Expansion program and could launch in the late 2020s. Should the current passive microwave sensors in orbit fail before these aforementioned European satellites are launched, gap filling data are currently available from the Feng Yun 3 (FY3) Microwave Radiation Imager (MWRI) operated by the Chinese Meteorological Administration (CMA).

376

377 **Glacier mass balance**

378

379 Variations in glacier mass are closely linked to changes in atmospheric forcing. The mass
380 balance of glaciers – defined as the sum of all gains and losses in ice mass – is primarily
381 affected by summer air temperatures. Variations in solid precipitation and radiation fluxes
382 also exert a significant influence on glacier mass change (Braithwaite, 1981; Ohmura, 2001).
383 Long-term cumulative glacier mass changes are thus a valuable indicator integrating the
384 effects of various components of the global climate system on snow and ice. As glaciers
385 adapt to altered climatic conditions by retreating to higher elevation, the mass change
386 signal also depends on their dynamic response. Glaciers are distributed over most
387 continents of the Earth with a concentration in the high mountain ranges of Asia, and
388 North/South America, as well as in high latitudes (Pfeffer et al., 2014). Limited glacierization
389 is however also present in tropical regions.

390

391 Observing the mass change of the roughly 200,000 glaciers outside the two ice sheets in
392 Greenland and Antarctica is challenging due to their remoteness and general inaccessibility
393 on the one hand, meaning that sampling of these glaciers is incomplete, and on the other
394 hand due to the inherent difficulty of directly measuring variations in glacier mass.
395 Therefore, a combination of different methodologies is employed. Direct field observations
396 on about 300 glaciers globally deliver data on seasonal to annual glacier mass change (Zemp
397 et al., 2015). Due to logistical reasons, most observations refer to glaciers smaller than
398 about 20 km^2, although in several regions larger glaciers are also monitored. Although at
399 least one series is available in all large-scale glacierized regions worldwide, measurements

400 are overrepresented in the European Alps, Scandinavia and the Rocky Mountains. Due to
401 the inhomogeneity of national monitoring programmes and the laborious field data
402 processing, global-scale results on seasonal or annual mass change are typically only
403 available a few months up to a year after acquisition. Comparison of repeated digital
404 elevation models of the ice surface, referred to as the geodetic method, allows assessing the
405 volume change of large glacier samples at time intervals of a few years to decades (e.g. Kääb
406 et al., 2012; Brun et al., 2017; Braun et al., 2019). The Gravity Recovery And Climate
407 Experiment (GRACE) provided a powerful method to directly observe glacier mass change
408 from space, albeit only at a spatial resolution of 100 km or more until its cessation in 2017.
409 Furthermore, uncertainties for mountain ranges with small glaciers are high due to
410 limitations in the model separating mass change signals from glaciers and other components
411 of the hydrological cycle (e.g., Gardner et al., 2013; Wouters et al., 2019).
412
413 Data on glacier mass balance (Figure 5) are collected through a worldwide network of
414 national correspondents and principal investigators and are further distributed by the World
415 Glacier Monitoring Service (WGMS, www.wgms.ch). Analysis of long-term variations in
416 glacier mass often relies on a set of global reference glaciers, being defined as sites with
417 continuous high-quality *in-situ* observations of more than 30 years. Results from these
418 series are, however, only partly representative for glacier mass changes at the global scale
419 as they are disproportionately in well-accessible regions (e.g. Europe). For the most recent
420 pentad 2015-2019, data of WGMS reference glaciers indicate specific mass-change rates
421 that are more negative than in all other periods since 1950 (Fig. 5a). These measurements
422 corroborate the widespread and substantial glacier mass losses recognized for several
423 decades.

Accepted for publication in *Bulletin of the American Meteorological Society.* DOI 10.1175/BAMS-D-19-0196.1.

Global mass change estimates require extrapolation of the scattered direct observations to all glaciers. The study by Zemp et al. (2019) provides a comprehensive assessment of glacier mass changes at the global scale based on a combination of year-to-year variabilities stemming from *in-situ* measurements, and decadal-scale geodetic mass changes from a large set of roughly 20,000 individual glaciers covering about 25% of the global glacier area. Results indicate an acceleration of glacier mass losses from around 1985, after moderately negative values (Fig. 5b). Over the last decade, glaciers lost more than 300 Gt yr^{-1} on average, thus approaching a sea-level rise contribution of 1 mm per year (Zemp et al., 2019). Mass loss from glaciers outside the two ice sheets thus makes up almost a third of the current sea-level rise. The glacier mass-change rates for the last decade are also confirmed by global studies based on satellite gravity and altimetry (Fig. 5b; Gardner et al., 2013; Wouters et al., 2019).

Knowledge on glacier mass change is limited before the 1960s. Only very few direct observations exist, and the spatial coverage of these measurements does not allow any global assessment. However, observations of glacier length change reaching back until the 16^{th} century in some cases (LeClercq et al., 2014), as well as glacier modelling (e.g., Marzeion et al., 2014) indicates significant glacier mass losses globally since the maximum of the so-called Little Ice Age around 1850. This is also consistent with geomorphological evidence (Grove, 2004).

Ocean acidification

Increasing atmospheric carbon dioxide concentrations affect the chemistry of the ocean. The ocean absorbs around 30% of the annual emissions of carbon dioxide (CO_2) to the atmosphere, which helps to alleviate the impacts of climate change on the planet. The CO_2 reacts with seawater and alters the acidity of the ocean by decreasing its pH. This process is called ocean acidification. The change of pH level is linked to a range of shifts in other carbonate chemistry parameters in the seawater, such as a decrease in carbonate ion concentrations. This lowers the saturation state of biogenic calcium carbonate minerals, including calcite and aragonite, used in the formations of shells and skeletal material by a variety of marine organisms, from mussels and crustaceans to corals, decreasing their ability to calcify (e.g., reef building corals and shelled molluscs). Together, the changes in CO_2 concentration, pH and carbonate chemistry parameters affect the energy budget of marine life, lessening the potential to grow and reproduce. It is therefore important to fully characterize the ocean's changing carbonate system through observations with high temporal and spatial resolution.

Ocean acidification observations started at a limited number of stations 30 years ago, a very limited set of observations compared with the other headline indicators, and at present data are generally reported at the station level rather than as a consolidated global indicator. Established methodology and standards are available, but data are not regularly produced by countries. IPCC (2019a) reported information on ocean pH based on eight stations globally with 15 years or more of data.

Notwithstanding the limited existing data, increasing awareness, international collaboration, e.g., that supported by the Intergovernmental Oceanographic Commission – United Nations Educational, Scientific and Cultural Organization (IOC-UNESCO), the Ocean Acidification International Coordination Centre (OA-ICC) and in particular the Global Ocean Acidification Observing Network (GOA-ON), and related capacity development activities have increased the human and technical capacity to measure ocean acidification and analyse related data sets. In 2015, ocean acidification was further identified as one topic to address within the 2030 Agenda for Sustainable Development (United Nations, 2015b) (Sustainable Development Goal (SDG) target 14.3). In 2017 UN Member States further agreed on the related indicator 14.3.1: *Average marine acidity (pH) measured at agreed suite of representative sampling stations.* IOC-UNESCO is the custodian agency for this SDG indicator, which means it is responsible to develop internationally agreed upon standards, coordinate the indicator development, and support increased adoption and compliance with the internationally agreed standards at the national level. Based on this methodology, IOC-UNESCO collects ocean acidification data from countries (or regional organizations) through existing mandates and reporting mechanism to provide internationally comparable data and calculate global and regional aggregates. The Commissions also strengthen national statistical capacity and improve reporting mechanisms for ocean acidification with specific capacity training activities. As a result of these initiatives, it is expected that the observation network for ocean acidification will expand rapidly over the next few years.

Accepted for publication in *Bulletin of the American Meteorological Society.* DOI 10.1175/BAMS-D-19-0196.1.

In 2019, a new 14.3.1 data portal[1] was launched by IOC-UNESCO, which now facilitates the reporting and analysis of ocean acidification dataand metadata towards reporting of the indicator. In turn, a headline indicator on ocean acidification can benefit from the collected data on an annual basis by IOC-UNESCO, assuring a high quality of scientific data and information used across different reporting mechanisms, international conventions and related publications/outputs.

Greenhouse gas concentration

Carbon dioxide is the single most important anthropogenic greenhouse gas in the atmosphere, contributing ~66% of the radiative forcing by long lived greenhouse gases. It is responsible for about 82% of the increase in radiative forcing over the past decade and about 81% of the increase over the past five years. Atmospheric concentration of CO_2 is closely linked to anthropogenic activities and it is defined by the exchange processes between the atmosphere, the biosphere and the oceans.

The long-term trends and seasonal variations in the global average mole fractions of CO_2 (Figure 6) are calculated using surface observations at stations of the Global Atmosphere Watch (GAW) Programme and its contributing networks. In total 129 stations were used for the calculation of the 2018 global average. For the global analysis (WMO, 2009) used in the WMO Greenhouse Gas Bulletin, stations were selected to be representative of their region

[1] www.goa-on.org.

513 and not significantly impacted by local CO_2 sources or sinks (for example, not impacted by
514 direct emissions from the traffic or industry or direct CO_2 uptake by the forest).

515 Data from the network are submitted to the WMO World Data Center for Greenhouse
516 Gases within eight months after the end of the calendar year, after receiving a thorough
517 quality control by the laboratories performing the measurements. Some stations provide
518 data on their websites in shorter release cycles with delays up to just one day, bypassing
519 part of the quality protocols, but only the fully quality controlled data can be used for the
520 global mean calculations.

521 All WMO GAW greenhouse gas observations are performed following the recommendation
522 for quality assurance, in particular the confirmed traceability chain to the primary WMO
523 scale, as described in WMO (2018b). To ensure global compatibility of the measurements,
524 the World Calibration Center (WCC), supported by NOAA, organizes regular comparisons in
525 which the set of the well-characterized cylinders is sent by the world calibration centre to
526 the stations in the chain (so that stations measure the same flasks one after the other). This
527 demonstrates the compatibility of the measurement systems.[2]

528 Selection of observational sites is based on whether they provide data representing a
529 reasonably large geographical area, considering the fact that some sites may be susceptible
530 to local emission sources and sinks.

531 The mole fractions of greenhouse gases exhibit variations on different time scales. The two
532 major components are seasonal variation and long-term trends. In the WMO Greenhouse

[2] Results can be found on the WCC web site https://www.esrl.noaa.gov/gmd/ccgg/wmorr/wmorr_results.php

Accepted for publication in *Bulletin of the American Meteorological Society.* DOI 10.1175/BAMS-D-19-0196.1.

Gas Bulletin, average seasonal variations derived from components of Fourier harmonics and long-term trends are extracted via a Lanczos low-pass filter.

In general, the number and distribution of sites used to assess trends during the analysis period should be kept unchanged as much as possible to avoid biases and additional uncertainties arising from introduction of the new data of removal of stations. However, data covering the entire analysis period are available for fewer than 20 sites[3]; for most sites, coverage is for shorter periods or contains data gaps. Smaller gaps are filled using linear interpolation based on available data in the fitted long-term trends derived by subtracting the average seasonal variation.

Six zonal mean mole fractions are calculated by determining the arithmetic average of the mole fractions in each latitudinal zone (90° to 60°, 60° to 30° and 30° to 0° in each hemisphere), based on consistent datasets derived as above. Global and hemispheric means are calculated as the weighted averages of the zonal means taking account of the area of each latitudinal zone. Growth rates for the whole globe, each hemisphere and each latitudinal zone are derived from the time derivatives of the corresponding long-term trends fitted to the observations (WMO, 2009). The uncertainty in global mean mole fractions (at a 68% confidence level) is calculated using bootstrap analysis. From the dataset of mole fractions obtained after the site selection and data extension procedure described above, *n* sites are randomly selected, with duplication of the same sites allowed on condition that at least one site is selected from each of the six latitudinal bands, and a global mean mole fraction is calculated using the data from the *n* sites. The procedure is repeated *m* times to

[3] https://gaw.kishou.go.jp/publications/summary

Accepted for publication in *Bulletin of the American Meteorological Society.* DOI 10.1175/BAMS-D-19-0196.1.

554 determine *m* different global mean mole fractions. Uncertainty is defined as the standard
555 deviation of these mole fractions.

556 The preindustrial levels of CO_2 are estimated with the same techniques as are used for
557 modern in situ measurements but using analysis of the air trapped in ice cores. Those levels
558 are estimated with a level of confidence which is lower than for modern observations
559 (uncertainty of the global mean estimate is 0.1 ppm), but still high (Marcott et al., 2014).
560 The 1750 globally averaged abundance of atmospheric CO_2 based on measurements of air
561 extracted from ice cores and from firn is 278 ± 2 ppm (Etheridge et al., 1996).

562

563 **Examples of variables not included in the key indicators**

564

565 An important characteristic of the indicators selected is that they represent variables which
566 can be expressed as a single number which is scientifically meaningful as an indicator of the
567 state of the climate system. Some important variables in the climate system were not
568 selected for the key indicators because they are not amenable to such a "single number"
569 expression, or because they lack the global coverage necessary to be considered fully
570 representative.

571

572 To illustrate these challenges, the question of whether the world is experiencing an
573 intensification of the hydrological cycle is an important one in assessing climate change. At
574 first glance, the most obvious indicator to report this would appear to be globally averaged
575 precipitation, which was one of the indicators originally under consideration (WMO, 2017a).
576 However, whereas for most key climate indicators, most parts of the world are changing in

Accepted for publication in *Bulletin of the American Meteorological Society.* DOI 10.1175/BAMS-D-19-0196.1.

the same direction, for precipitation, there are strong regional variations in the sign of observed changes (IPCC, 2013), making regional signals of greater importance for many applications than an overall global signal.

Globally averaged precipitation on land is reported annually from a number of different data sets (Vose et al., 2018), whilst precipitation over the ocean, using satellite data alongside in situ observations is also reported from the satellite-based Global Precipitation Climatology Project (GPCP) data set (Huffman et al., 2009). However, the spread between the land-based data sets is large in both historical (Herold et al., 2016; Gehne et al., 2016) and recent data - for example, the 2017 mean annual global precipitation over land reported in Vose et al. (2018) ranged from only slightly above average to the highest on record – whilst data over the ocean are only available during the satellite era. Reanalysis precipitation data sets also show a large degree of divergence (Alexander et al., 2020). Interannual variations in the distribution of precipitation over land and ocean are also strongly influenced by seasonal climate drivers (Gu and Adler, 2011), such as the El Niño-Southern Oscillation (ENSO), as well as longer-term forcings, complicating interpretation of global or semi-global means.

The seven headline indicators all reflect mean-state variables measured at seasonal and/or annual timescales. Many of the most significant impacts of climate change occur as a result of extreme events. It would be desirable, in that context, to include an indicator of the occurrence of extreme events as a key headline indicator. However, at present, the spatial coverage of routine reporting of extremes indices, such as the indices of temperature and precipitation extremes defined by the Expert Team on Climate Change Detection and Indices (ETCCDI), is limited, with recent analyses largely confined to Europe, North America,

Accepted for publication in *Bulletin of the American Meteorological Society.* DOI 10.1175/BAMS-D-19-0196.1.

Australia and parts of Asia (Perkins-Kirkpatrick et al., 2018; Tye et al., 2018; Figure 7). This is largely due to the lack of a mechanism for routine reporting of the daily temperature and precipitation data needed for the calculation of these indices, combined with limited exchange of historical daily data, and limited updating of the indices data sets developed for many parts of the world in the 2000s through the ETCCDI series of workshops (Peterson and Manton, 2008). WMO has recently introduced provisions for quality-controlled daily data to be exchanged routinely through the monthly CLIMAT messages and it is hoped that strong uptake of this will improve the capacity to monitor extremes in a timely manner, opening the possibility of regular reporting of one or more globally measured indicators of climate extremes in the future. Some use is also beginning to be made of reanalyses for reporting of indices of climate extremes (King et al., 2019).

Future opportunities and challenges

Observations are important for understanding the current trajectory of climate change. Global mean surface temperature is a key indicator used in the Paris Agreement, whilst the seven key indicators, along with other ECVs, are widely used in assessing whether observed climate change is consistent with model projections.

Our capacity to observe most of the variables used for assessment of the key climate indicators is improving over time. The introduction of Argo and related systems have greatly enhanced the monitoring of ocean-based indicators (e.g. Johnson et al., 2019), whilst remote sensing platforms have also made possible forms of monitoring which would not

have been practical with traditional in situ measurements. Reanalyses also play an increasingly important role in operational climate monitoring products such as the WMO State of the Global Climate report and contribute to regular reporting of GMST. In situ measurements are still very important to the global observing system and are critical for assessment of global temperatures and greenhouse gas concentrations.

Maintenance of observing platforms is a constant challenge. As noted for sea ice extent, important data sources can be vulnerable to individual satellites reaching the end of their expected lifespan or otherwise failing without adequate replacement. *In situ* networks are also regularly under pressure, especially in data-sparse regions such as Africa, parts of Asia, and South and Central America. Effective management of the data which are collected, and their transmission through channels from which they can be incorporated into global data sets, are also important.

In parallel with the designation of headline climate indicators, WMO is introducing a framework for the assessment of the maturity of climate data sets incorporating ECVs[4]. A number of data set providers have submitted their data sets for assessment. This process is still in the early stages of implementation and the fact that a specific data set has not yet been assessed should not be considered as an indication that it is inferior to those data sets which have been assessed. There is also a need for harmonized standards for data reporting and metadata for balanced assessment of the indicators.

[4] https://climatedata-catalogue.wmo.int/about

Acknowledgements

MDP was supported by the Met Office Hadley Centre Climate Programme funded by BEIS and Defra (United Kingdom).

References

Abraham, J. P., and Coauthors, 2013: A review of global ocean temperature observations: Implications for ocean heat content estimates and climate change, *Rev. Geophys.*, **51**, 450–483, https://doi.org/10.1002/rog.20022.

Abram, N.J., E.W. Wolff and M.A.J. Curran, 2013: A review of sea ice proxy information from polar ice cores. *Quaternary Science Reviews*, **79**, 168–183, https://doi.org/10.1016/j.quascirev.2013.01.011.

Alexander, L. V., M. Bador, R. Roca, S. Contractor, M. G. Donat and P. L. Nguyen, 2020: Intercomparison of annual precipitation indices and extremes over global land areas from *in situ*, space-based and reanalysis products. *Env. Res. Lett.*, in press, https://doi.org/10.1088/1748-9326/ab79e2.

Allen, M.R., O. P. Dube, W. Solecki, F. Aragón-Durand, W. Cramer, S. Humphreys, M. Kainuma, J. Kala, N. Mahowald, Y. Mulugetta, R. Perez, M. Wairiu, and K. Zickfeld, 2018:

Accepted for publication in *Bulletin of the American Meteorological Society.* DOI 10.1175/BAMS-D-19-0196.1.

Framing and Context. In: *Global Warming of 1.5°C. An IPCC Special Report on the impacts of global warming of 1.5°C above pre-industrial levels and related global greenhouse gas emission pathways, in the context of strengthening the global response to the threat of climate change, sustainable development, and efforts to eradicate poverty* [Masson-Delmotte, V., P. Zhai, H.-O. Pörtner, D. Roberts, J. Skea, P.R. Shukla, A. Pirani, W. Moufouma-Okia, C. Péan, R. Pidcock, S. Connors, J.B.R. Matthews, Y. Chen, X. Zhou, M.I. Gomis, E. Lonnoy, T. Maycock, M. Tignor, and T. Waterfield (eds.)].

Blunden, J., D. S. Arndt and G. Hartfield, eds., 2018: State of the Climate in 2017. *Bull. Amer. Meteor. Soc.*, **99**, Si–S310, http://doi.org/10.1175/2018BAMSStateoftheClimate.I.

Bojinski, S., Verstraete, M., Peterson, T.C., Richter, C., Simmons, A. and Zemp, M. 2014. The concept of essential climate variables in support of climate research, applications, and policy. *Bull. Amer. Meteor. Soc.*, **95**, 1431–1443, https://doi.org/10.1175/BAMS-D-13-00047.1.

Boyer, T., C.M. Domingues, S.A. Good, G.C. Johnson, J.M. Lyman, M. Ishii, V. Gouretski, J.K. Willis, J. Antonov, S. Wijffels, J.A. Church, R. Cowley, and N.L. Bindoff, 2016: Sensitivity of Global Upper-Ocean Heat Content Estimates to Mapping Methods, XBT Bias Corrections, and Baseline Climatologies. *J. Climate*, **29**, 4817–4842, https://doi.org/10.1175/JCLI-D-15-0801.1

Braun, M. H., P. Malz, C. Sommer, D. Farías-Barahona, T. Sauter, G. Casassa, A. Soruco, P. Skvarca and T. C. Seehaus, 2019: Constraining glacier elevation and mass changes in South America. *Nature Climate Change*, **9**, 130–136, https://doi.org/10.1038/s41558-018-0375-7.

Braithwaite, R. J., 1981: On glacier energy balance, ablation, and air temperature. *J. Glaciology*, **27**, 381–391, https://doi.org/10.3189/S0022143000011424.

Accepted for publication in *Bulletin of the American Meteorological Society.* DOI 10.1175/BAMS-D-19-0196.1.

694 Brun, F., E. Berthier, P. Wagnon, A. Kääb and D. Treichler, 2017: A spatially resolved
695 estimate of High Mountain Asia glacier mass balances from 2000 to 2016. *Nature Geosci.*,
696 **10**, 668−673, https://doi.org/10.1038/ngeo2999.
697 Cazenave, A. and Coauthors. 2019. Observational requirements for long-term monitoring of
698 the global mean sea level and its components over the altimetry era. *Frontiers in Marine*
699 *Science*, **6**, 582. https://doi.org/10.3389/fmars.2019.00582.
700 Cheng, L. and Coauthors, 2016: XBT Science: Assessment of Instrumental Biases and Errors.
701 *Bull. Amer. Meteor. Soc.*, **97**, 924–933, https://doi.org/10.1175/BAMS-D-15-00031.1
702 Cheng, L., K. E. Trenberth, J. Fasullo, T. Boyer, J. Abraham and J. Zhu, 2017: Improved
703 estimates of ocean heat content from 1960 to 2015. *Science Advances*, **3**, E1601545.
704 https://doi.org/10.1126/sciadv.1601545
705 Comiso, J. C., W. N. Meier, and R. Gersten, 2017: Variability and trends in the Arctic Sea ice
706 cover: Results from different techniques. *J. Geophys. Res.-Oceans*, **122**, 6883–6900,
707 https://doi.org/10.1002/2017JC012768
708 Cowtan, K. and R. G. Way, 2014: Coverage bias in the HadCRUT4 temperature series and its
709 impact on recent temperature trends. *Q. J. Roy. Meteor. Soc.*, **140**, 1935−1944.
710 https://doi.org/10.1002/qj.2297.
711 Davy, R., L. Chen, and E. Hanna, 2018: Arctic amplification metrics. *Int. J. Climatol.*, **38**,
712 4384−4394. https://doi.org/10.1002/joc.5675.
713 Desbruyères, D.G., S. G. Purkey, E. L. McDonagh, G. C. Johnson and B. A. King, 2016: Deep
714 and abyssal ocean warming from 35 years of repeat hydrography. *Geophys. Res. Lett.*
715 , **43**, 10356−10365. https://doi.org/10.1002/2016gl070413

716 Desbruyères, D., E.L. McDonagh, B.A. King, and V. Thierry, 2017: Global and Full-Depth
717 Ocean Temperature Trends during the Early Twenty-First Century from Argo and Repeat
718 Hydrography. *J. Climate*, **30**, 1985–1997, https://doi.org/10.1175/JCLI-D-16-0396.1
719 Donat, M.G., L. V. Alexander, H. Yang, I. Durre, R. Vose and J. Caesar, 2013: Global land-
720 based datasets for monitoring climate extremes. *Bull. Amer. Meteor. Soc.*, **94**, 997−1006,
721 https://doi.org/ 10.1175/BAMS-D-12-00109.1.
722 Eisenman, I., W. N. Meier and J. R. Norris, 2014: A spurious jump in the satellite record: has
723 Antarctic sea ice expansion been overestimated?, *The Cryosphere*, **8**, 1289–1296,
724 https://doi.org/10.5194/tc-8-1289-2014.
725 Etheridge, D. M., L. P. Steele, R. L. Langenfelds, R. J. Francey, J-M. Barnola, and V. I. Morgan,
726 1996. Natural and anthropogenic changes in atmospheric CO2 over the last 1000 years from
727 air in Antarctic ice and firn. *J. Geophys. Res.*, **101**, 4115−4128.
728 https://doi.org/10.1029/95JD03410
729 Fetterer, F., K. Knowles, W. N. Meier, M. Savoie, and A. K. Windnagel, 2017: Sea Ice Index,
730 Version 3. Boulder, Colorado USA. NSIDC: National Snow and Ice Data Center.
731 https://doi.org/10.7265/N5K072F8.
732 Freeman, E. and Coauthors, 2017: ICOADS Release 3.0: a major update to the historical
733 marine climate record. *Int. J. Climatol.*, **37**, 2211−2232. https://doi.org/10.1002/joc.4775.
734 Gallaher, D.W., G. G. Campbell and W. N. Meier, 2014: Anomalous variability in Antarctic sea
735 ice extents during the 1960s with the use of Nimbus data. *IEEE Journal of Selected*
736 *Topics in Applied Earth Observations and Remote Sensing*, **7**, 881–887. https://doi.
737 org/10.1109/JSTARS.2013.2264391.
738 Gardner, A. S. and Coauthors, 2013: A reconciled estimate of glacier contributions to sea
739 level rise: 2003 to 2009. *Science*, **340**, 852−857, https://doi.org/10.1126/science.1234532

Accepted for publication in *Bulletin of the American Meteorological Society.* DOI 10.1175/BAMS-D-19-0196.1.

740 Gehne, M., T. M. Hamill, G. N. Kiladis and K. E. Trenberth, 2016: Comparison of global
741 precipitation estimates across a range of temporal and spatial scales. *J. Climate*, **29**,
742 7773−7795.
743 Gill, A., 1982: *Atmosphere-Ocean Dynamics*. Academic Press, New York, 662 pp.
744 Good, S. A., M. J. Martin and N. A. Rayner, 2013: EN4: Quality Controlled Ocean
745 Temperature and Salinity Profiles and Monthly Objective Analyses With Uncertainty
746 Estimates, *J. Geophys. Res. - Oceans*, **118**, 6704−6716, https://doi.org/
747 10.1002/2013JC009067
748 Global Climate Observing System. 2017. Indicators of climate change: outcome of a meeting
749 held at WMO 3 February 2017. *GCOS No. 206,* World Meteorological Organization, Geneva,
750 29 pp. Available at https://library.wmo.int/doc_num.php?explnum_id=3418.
751 Grove, J. M., 2004: *Little ice ages: ancient and modern (Vol. 1)*. Taylor and Francis, 402 pp.
752 Gu, G. and R. F. Adler, 2011: Precipitation and temperature variations on the interannual
753 time scale: assessing the impact of ENSO and volcanic eruptions. *J. Climate*, **24**, 2258−2270,
754 https://doi.org/ 10.1175/2010JCLI3727.1.
755 Hawkins, E. and Coauthors, 2017: Estimating changes in global temperature since the
756 preindustrial period. *Bull. Amer. Meteor. Soc.*, **98**, 1841−1856. https://doi.org/
757 10.1175/BAMS-D-16-0007.1.
758 Herold, N., L. V. Alexander, M. G. Donat, S. Contractor and A. Becker, 2016: How much does
759 it rain over land? *Geophys. Res. Lett.*, **43**, 341−348, https://doi.org/ 10.1002/2015GL066615.
760 Hobbs, W.R., R. Massom, S. Stammerjohn, P. Reid, G. Williams and W. Meier, 2016: A review
761 of recent changes in Southern Ocean sea ice, their drivers and forcings. *Global and Planetary*
762 *Change*, **143**, 228–250, https://doi.org/10.1016/j.gloplacha.2016.06.008.

Accepted for publication in *Bulletin of the American Meteorological Society.* DOI 10.1175/BAMS-D-19-0196.1.

763 Horwath, M., and Coauthors, 2020: *ESA Climate Change Initiative (CCI) Sea Level Budget*
764 *Closure (SLBC_cci) Summary Report D4.2*. Version 1.0, 09.03.2020.

765 Huffman, G.J., R. F. Adler, D. T. Bolvin and G. Gu, 2009: Improving the global precipitation
766 record: GPCP version 2.1. *Geophys. Res. Lett.,* **36**, L17808, https://doi.org/
767 10.1029/2009GL040000.

768 IPCC, 2013: *Climate Change 2013: The Physical Science Basis. Contribution of Working Group*
769 *I to the Fifth Assessment Report of the Intergovernmental Panel on Climate Change*.
770 [Stocker, T.F., D. Qin, G.-K. Plattner, M. Tignor, S.K. Allen, J. Boschung, A. Nauels, Y. Xia, V.
771 Bex and P.M. Midgley (eds.)]. Cambridge University Press, Cambridge, United Kingdom and
772 New York, USA, 1585 pp.

773 IPCC, 2019a: *IPCC Special Report on the Ocean and Cryosphere in a Changing Climate* [H.-O.
774 Pörtner, D.C. Roberts, V. Masson-Delmotte, P. Zhai, M. Tignor, E. Poloczanska, K.
775 Mintenbeck, A. Alegría, M. Nicolai, A. Okem, J. Petzold, B. Rama, N.M. Weyer (eds.)]. In
776 press.

777 IPCC, 2019b: *Climate Change and Land: an IPCC special report on climate change,*
778 *desertification, land degradation, sustainable land management, food security, and*
779 *greenhouse gas fluxes in terrestrial ecosystems* [P.R. Shukla, J. Skea, E. Calvo Buendia, V.
780 Masson-Delmotte, H.-O. Pörtner, D. C. Roberts, P. Zhai, R. Slade, S. Connors, R. van Diemen,
781 M. Ferrat, E. Haughey, S. Luz, S. Neogi, M. Pathak, J. Petzold, J. Portugal Pereira, P. Vyas, E.
782 Huntley, K. Kissick, M. Belkacemi, J. Malley, (eds.)]. In press.

783 Ivanova, N. and Coauthors, 2015: Inter-comparison and evaluation of sea ice algorithms:
784 towards further identification of challenges and optimal approach using passive microwave
785 observations. *The Cryosphere*, **9**, 1797–1817, https://doi.org/10.5194/tc-9-1797-2015

Accepted for publication in *Bulletin of the American Meteorological Society.* DOI 10.1175/BAMS-D-19-0196.1.

786 Johnson, G. C. and Coauthors,]2019: Ocean heat content [in “State of the Climate in 2018”].
787 *Bull. Amer. Meteor. Soc.*, **100**, S74−77,
788 https://doi.org/10.1175/2019BAMSStateoftheClimate.1.
789 Kääb, A., E. Berthier, C. Nuth, J. Gardelle and Y. Arnaud, 2012: Contrasting patterns of early
790 twenty-first-century glacier mass change in the Himalayas. *Nature*, 488, 495−498,
791 https://doi.org/10.1038/nature11324.
792 Kennedy, J. J., N. A. Rayner, C. P. Atkinson and R. E. Killick, 2019: An Ensemble Data Set of
793 Sea Surface Temperature Change From 1850: The Met Office Hadley Centre HadSST.4.0.0.0
794 Data Set. *J. Geophys. Res. Atmos.*, **124**, 7719−7763, https://doi.org/10.1029/2018JD029867.
795 King, A. D., M. G. Donat and R. J. H. Dunn, 2019: Land surface temperature extremes [in
796 “State of the Climate in 2018”], *Bull. Amer. Met. Soc.*, **100**, S14−16,
797 http://doi.org/10.1175/2019BAMSStateoftheClimate.1.
798 Kinnard, C., C. M. Zdanowicz, D. A. Fisher, E. Isaksson, A. de Vernal and L. G. Thompson,
799 2011: Reconstructed changes in Arctic sea ice over the past 1,450 years. *Nature*, **479**, 509–
800 512, https://doi.org/10.1038/nature10581
801 Lavergne, T. and Coauthors, 2019: Version 2 of the EUMETSAT OSI SAF and ESA CCI sea-ice
802 concentration climate data records. *The Cryosphere*, **13**, 49−78, https://doi.org/10.5194/tc-
803 13-49-2019.
804 Leclercq, P. W., J. Oerlemans, H. J. Basagic, I. Bushueva, A. J. Cook and R. Le Bris, 2014: A
805 data set of worldwide glacier fluctuations. *The Cryosphere*, **8**, 659−672,
806 https://doi.org/10.5194/tc-8-659-2014.

807 Legeais J.F., and Coauthors, 2018: An improved and homogeneous altimeter sea level record
808 from the ESA Climate Change Initiative. *Earth Syst. Sci. Data*, **10**, 281−301,
809 https://doi.org/10.5194/essd-10-281-2018, 2018.
810 Lyman, J.M. and G.C. Johnson, 2008: Estimating Annual Global Upper-Ocean Heat Content
811 Anomalies despite Irregular In Situ Ocean Sampling. *J. Climate*, **21**, 5629–5641,
812 https://doi.org/10.1175/2008JCLI2259.1
813 Marcott, S. A. and Coauthors, 2014: Centennial-scale changes in the global carbon cycle
814 during the last deglaciation, Nature, **514**, 616−619, https://doi.org/10.1038/nature13799.
815 Marzeion, B., J. G. Cogley, K. Richter and D. Parkes, 2014: Attribution of global glacier mass
816 loss to anthropogenic and natural causes. *Science*, **345**, 919−921, https://doi.org/
817 10.1126/science.1254702.
818 Meier, W.N and J. J. Stewart, 2019: Assessing uncertainties in sea ice extent climate
819 indicators. *Environ. Res. Lett.*, **14**, 035005, https://doi.org/10.1088/1748-9326/aaf52c.
820 Meyssignac, B. and Coauthors, 2019: Measuring Global Ocean Heat Content to Estimate the
821 Earth Energy Imbalance. *Front. Mar. Sci.*, **6**, 432, https://doi.org/10.3389/fmars.2019.00432
822 Morice, C.P., J. J. Kennedy, N. A. Rayner and P. D. Jones, 2012: Quantifying uncertainties in
823 global and regional temperature change using an ensemble of observational estimates: the
824 HadCRUT4 data set. *J. Geophys. Res.*, **117**, D08101, https://doi.org/ 10.1029/2011JD017187.
825 Nerem, R. S., B. D. Beckley, J. Fasullo, B. D. Hamlington, D. Masters and G. T. Mitchum, 2018:
826 Climate Change Driven Accelerated Sea Level Rise Detected In The Altimeter Era. *Proc. Nat.*
827 *Acad. Sci.,* **15**, 2022-2025, https://doi.org/10.1073/pnas.1717312115
828 Ohmura, A., 2001: Physical basis for the temperature-based melt-index method. *J. Appl.*
829 *Meteor.*, **40**, 753−761, https://doi.org/10.1175/1520-0450(2001)040<0753:PBFTTB>
830 2.0.CO;2.

Accepted for publication in *Bulletin of the American Meteorological Society.* DOI 10.1175/BAMS-D-19-0196.1.

831 Palmer M. D., K. Haines, S. F. B. Tett and T. J. Ansell, 2007: Isolating the Signal of Global
832 Ocean Warming. *Geophys. Res. Lett.*, **34**, L23610, https://doi.org/10.1029/2007GL031712
833 Palmer, M. D. and P. Brohan, 2011: Estimating sampling uncertainty in fixed-depth and
834 fixed-isotherm estimates of ocean warming. *Int. J. Climatol.*, **31**, 980−986.
835 https://doi.org/10.1002/joc.2224
836 Palmer, M. D. and D. J. McNeall, 2014: Internal variability of Earth's energy budget
837 simulated by CMIP5 climate models, *Environ. Res. Lett.*, **9**, 034016,
838 https://doi.org/10.1088/1748-9326/9/3/034016
839 Palmer, M. D., 2017: Reconciling Estimates of Ocean Heating and Earth's Radiation Budget.
840 *Current Climate Change Reports*, **3**, 78–86. https://doi.org/10.1007/s40641-016-0053-7
841 Palmer, M. D. and Coauthors, 2017: Ocean heat content variability and change in an
842 ensemble of ocean reanalyses. *Climate Dynamics*, **49**, 909–930.
843 https://doi.org/10.1007/s00382-015-2801-0.
844 Parkinson, C.L., 2019: A 40-y record reveals gradual Antarctic sea ice increases followed by
845 decreases at rates far exceeding the rates seen in the Arctic. *Proc. Nat. Acad. Sci.*, **116**,
846 14414−14423, https://doi.org/ 10.1073/pnas.1906556116
847 Perkins-Kirkpatrick, S.E., M.G. Donat and R. J. H. Dunn, 2018: Land surface temperature
848 extremes [in "State of the Climate in 2017"]. *Bull. Amer. Meteor. Soc.*, 99, S15−S16,
849 https://doi.org/10.1175/2018BAMSStateoftheClimate.I.
850 Peterson, T.C. and M. J. Manton, 2008: Monitoring changes in climate extremes: a tale of
851 international cooperation. *Bull. Amer. Meteor. Soc.*, **89**, 1266−1271.
852 Pfeffer, W. T. and Coauthors, 2014: The Randolph Glacier Inventory: a globally complete
853 inventory of glaciers. *J. Glaciology*, **60**, 537−552, https://doi.org/10.3189/2014JoG13J176.

854 Purkey, S. G. and G. C. Johnson, 2010: Warming of Global Abyssal and Deep Southern Ocean
855 Waters between the 1990s and 2000s: Contributions to Global Heat and Sea Level Rise
856 Budgets. *J. Climate*, **23**, 6336–6351, https://doi.org/10.1175/2010JCLI3682.1
857 Riser, S. C. and Coauthors, 2016: Fifteen years of ocean observations with the global Argo
858 array. *Nature Climate Change*, **6**, 145–153. https://doi.org/10.1038/nclimate2872
859 Roemmich, D., W. J. Gould and J. Gilson, 2012: 135 years of global ocean warming between
860 the Challenger expedition and the Argo Programme. *Nature Climate Change*, **2**, 425–428.
861 https://doi.org/10.1038/nclimate1461
862 Simmons, A.J., P. Berrisford, D. P. Dee, H. Hersbach, S. Hirahara and J.-N. Thépaul, 2017: A
863 reassessment of temperature variations and trends from global reanalyses and monthly
864 surface climatological datasets. *Q. J. Roy. Meteor. Soc.,* **143**, 101−119. https://doi.org/
865 10.1002/qj.2949.
866 Tye, M.R., S. Blenkinsop, M. Donat, I. Durre and M. Ziese, 2018: Land surface precipitation
867 extremes [in "State of the Climate in 2017"]. *Bull. Amer. Meteor. Soc.*, **99**, S29−S31,
868 https://doi.org/10.1175/2018BAMSStateoftheClimate.I.
869 United Nations, 2015a: *Paris Agreement*. United Nations, New York, 27 pp., available at
870 https://unfccc.int/files/essential_background/convention/application/pdf/english_paris_agr
871 eement.pdf.
872 United Nations, 2015b: *Transforming our world: the 2030 agenda for sustainable*
873 *development*. United Nations, New York, 44 pp., available at
874 https://sustainabledevelopment.un.org/post2015/transformingourworld/publication.
875 von Schuckmann, K. and Coauthors, 2016: An imperative to monitor Earth's energy
876 imbalance, *Nature Climate Change*, **6**, 138–144, https://doi.org/10.1038/nclimate2876

877 von Schuckmann, K. and Coauthors, 2018: Copernicus Marine Service Ocean State Report, *J.*
878 *Operational Oceanogr.*, **11**, S1−S142, https://doi.org/10.1080/1755876X.2018.1489208
879 Vose, R.S., R. Adler, A. Becker and X. Yin, 2018: Precipitation [in "State of the Climate in
880 2017"]. *Bull. Amer. Meteor. Soc.*, **99**, S28−S31,
881 https://doi.org/10.1175/2018BAMSStateoftheClimate.I.
882 Walsh, J.E., F. Fetterer, J. S. Stewart and W.L. Chapman, 2017: A database for depicting
883 Arctic sea ice variations back to 1850. *Geog. Review*, **107**, 89–107,
884 https://doi.org/10.1111/j.1931-0846.2016.12195.x.
885 Wijffels, S. E., D. Roemmich, D. Monselesan, J. Church and J. Gilson, 2016: Ocean
886 temperatures chronicle the ongoing warming of Earth. Nature Climate Change, **6**,116−118,
887 https://doi.org/10.1038/nclimate2924
888 Williams, M. and S. Eggleston, 2017: Using indicators to explain our changing climate to
889 policymakers and the public. *WMO Bulletin*, **66 (2)**, 33−39.
890 Witze, A, 2017: Ageing satellites put crucial sea-ice climate record at risk. *Nature*, **551**,
891 13−14, https://doi.org/10.1038/nature.2017.22907
892 Wong, A., R. Keeley and T. Carval, 2018: *Argo Quality Control Manual For CTD and*
893 *Trajectory Data*. https://doi.org/10.13155/33951
894 World Climate Research Program (WCRP) Global Sea Level Budget Group, 2018: Global sea-
895 level budget 1993-present. *Earth Syst. Sci. Data*, **10**, 1551−1590.
896 https://doi.org/10.5194/essd-10-1551-2018.
897 World Meteorological Organization, 2009: Technical Report of Global Analysis Method for
898 Major Greenhouse Gases by the World Data Center for Greenhouse Gases (Y. Tsutsumi, K.
899 Mori, T. Hirahara, M. Ikegami and T.J.Conway). *GAW Report No. 184 (WMO/TD-No. 1473)*,

Accepted for publication in *Bulletin of the American Meteorological Society.* DOI 10.1175/BAMS-D-19-0196.1.

World Meteorological Organization, Geneva. Available at https://www.wmo.int/pages/prog/arep/gaw/documents/TD_1473_GAW184_web.pdf

World Meteorological Organization, 2015. *Status of the global observing system for climate*. World Meteorological Organization, Geneva, 373 pp.

World Meteorological Organization, 2017a. Expert meeting on the WMO Statements on the Status of the Global Climate: meeting report. *WCDMP No. 84*, World Meteorological Organization, Geneva, 18 pp. Available at https://www.wmo.int/pages/prog/wcp/wcdmp/documents/Report-Expert-meeting_final-WCDMP-84.pdf.

World Meteorological Organization, 2017b. WMO Guidelines on the Calculation of Climate Normals. *WMO No. 1203*, World Meteorological Organization, Geneva, 29 pp.

World Meteorological Organization, 2018a. Commission for Climatology: abridged final report of the Seventeenth Session. *WMO No. 1216*, World Meteorological Organization, Geneva, 57 pp. Available at https://library.wmo.int/doc_num.php?explnum_id=4611.

World Meteorological Organization, 2018b: 19th WMO/IAEA Meeting on Carbon Dioxide, Other Greenhouse Gases and Related Measurement Techniques (GGMT-2017). *Technical publications GAW Report- No. 242*, World Meteorological Organization, Geneva. Available at https://library.wmo.int/doc_num.php?explnum_id=5456

World Meteorological Organization, 2018c: *WMO Statement on the state of the global climate in 2017*. World Meteorological Organization, Geneva.

World Meteorological Organization. 2019. *WMO Statement on the state of the global climate in 2018*. World Meteorological Organization, Geneva.

Wouters, B., A.S. Gardner and G. Moholdt, 2019: Status of the global glaciers from GRACE (2002-2016). *Frontiers in Earth Science*, **7**, 75.

Accepted for publication in *Bulletin of the American Meteorological Society.* DOI 10.1175/BAMS-D-19-0196.1.

924 Zanna, L., S. Khatiwala, J.M. Gregory, J. Ison and P. Heimbach, 2019: Global reconstruction of
925 historical ocean heat storage and transport. *Proc. Nat. Acad. Sci.*, **116**, 1126−1131.
926 https://doi.org/10.1073/pnas.1808838115
927 Zemp, M. and Coauthors, 2015: Historically unprecedented global glacier decline in the early
928 21st century. *J. Glaciology*, **61**, 745−762, https://doi.org/10.3189/2015JoG15J017.
929 Zemp, M. and Coauthors, 2019: Global glacier mass changes and their contributions to sea-
930 level rise from 1961 to 2016. *Nature*, **568**, 382−386, https://doi.org/10.1038/s41586-019-
931 1071-0.

932
933 **Tables**
934

Category	Sub-category	Essential Climate Variables
Atmospheric	Surface	Precipitation; pressure; temperature; surface radiation budget; wind speed and direction; water vapour
	Upper atmosphere	Earth radiation budget; lightning; temperature; water vapour; wind speed and direction
	Atmospheric composition	Aerosols properties; carbon dioxide, methane and other greenhouse gases; cloud properties; ozone; precursors (supporting the aerosols and ozone ECVs)
Oceanic	Physics	Ocean surface heat flux; sea ice; sea level; sea state; sea surface salinity; sea surface temperature; subsurface currents; subsurface salinity; subsurface temperature; surface currents; surface stress
	Biogeochemistry	Inorganic carbon; nitrous oxide; nutrients; ocean colour; oxygen; transient tracers
	Biology/ecosystems	Marine habitat properties; plankton
Terrestrial		Above-ground biomass; albedo; anthropogenic greenhouse gas fluxes; anthropogenic water use; fire; fraction of absorbed photosynthetically active radiation (FAPAR); glaciers; groundwater; ice sheets and ice shelves; lakes; land cover; land surface temperature; latent and sensible heat fluxes; leaf area index (LAI); permafrost; river discharge; snow; soil carbon; soil moisture

935
936 Table 1. The current Essential Climate Variables.
937

Accepted for publication in *Bulletin of the American Meteorological Society.* DOI 10.1175/BAMS-D-19-0196.1.

Variable	Proposed indicator
Temperature	Global mean surface temperature
Ocean heat content	Global ocean heat content anomaly
Sea level	Global mean sea level change from a reference benchmark
Sea ice extent	Sea ice extent for the Arctic and Antarctic
Glacier mass balance	Global mass change of glaciers outside the Greenland and Antarctic ice sheets
Ocean acidification	Global mean ocean pH
Greenhouse gas mole fractions	Mean global mole fraction of CO_2

Table 2. The seven headline climate indicators

Accepted for publication in *Bulletin of the American Meteorological Society.* DOI 10.1175/BAMS-D-19-0196.1.

948
949
950
951

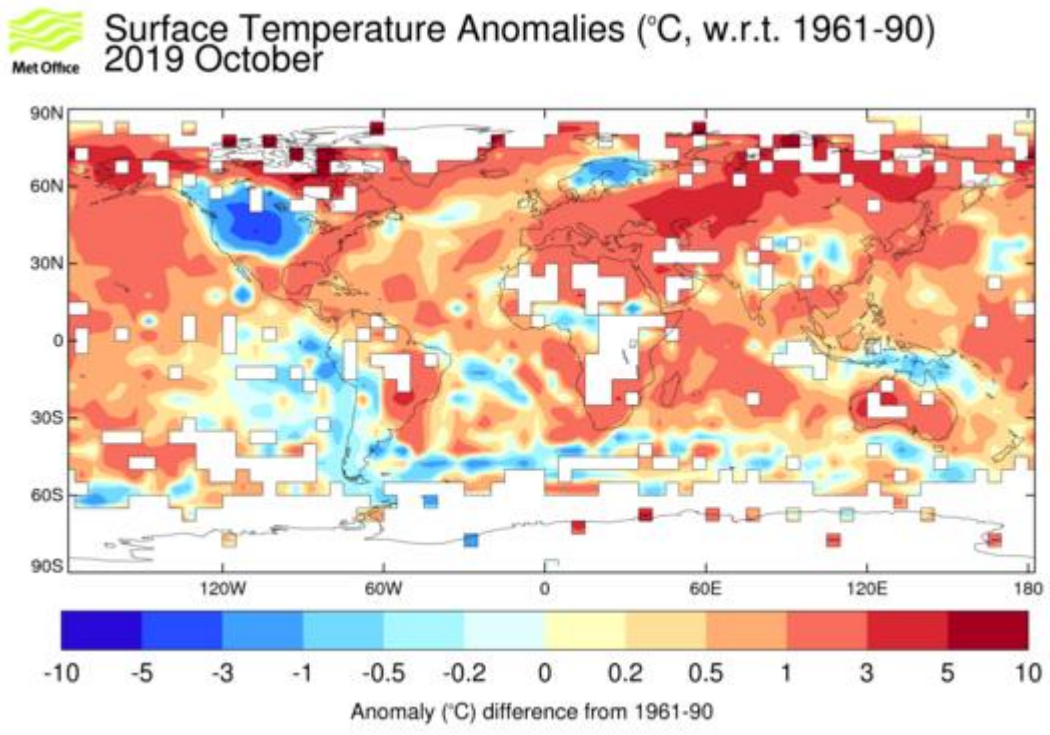

952

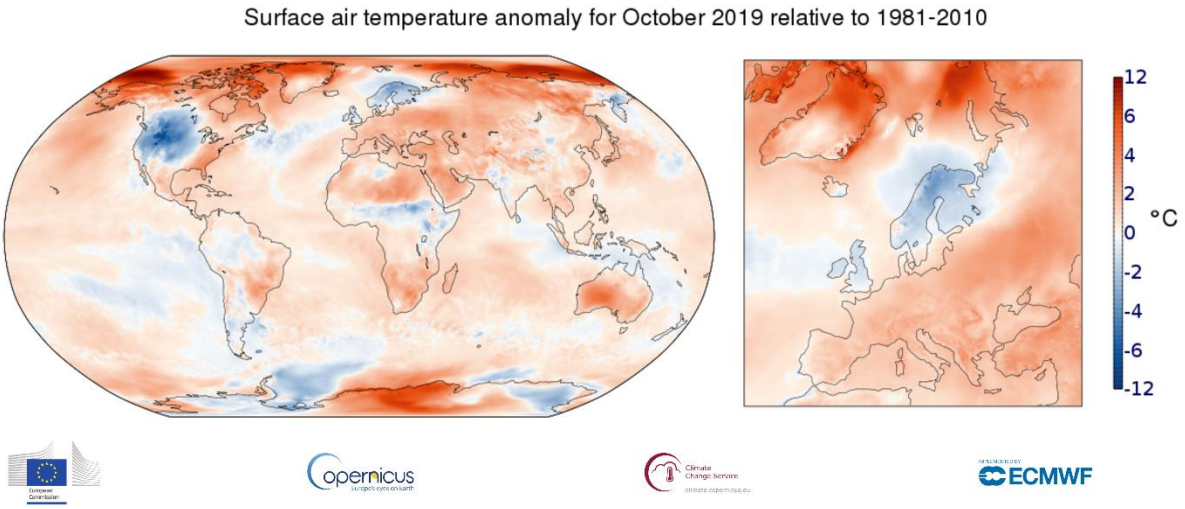

953
954 Figure 1. October 2019 global temperature anomaly (°C) maps showing differing coverage in
955 different data sets: (a) the HadCRUT4 data set (United Kingdom Meteorological Office) (b)
956 the ERA5 reanalysis (Copernicus Climate Change Service/ECMWF). The ERA5 data set shows
957 more extensive coverage in polar regions, and over Africa, than does HadCRUT4. This also

illustrates the different baseline periods used by different data providers in their routine products.

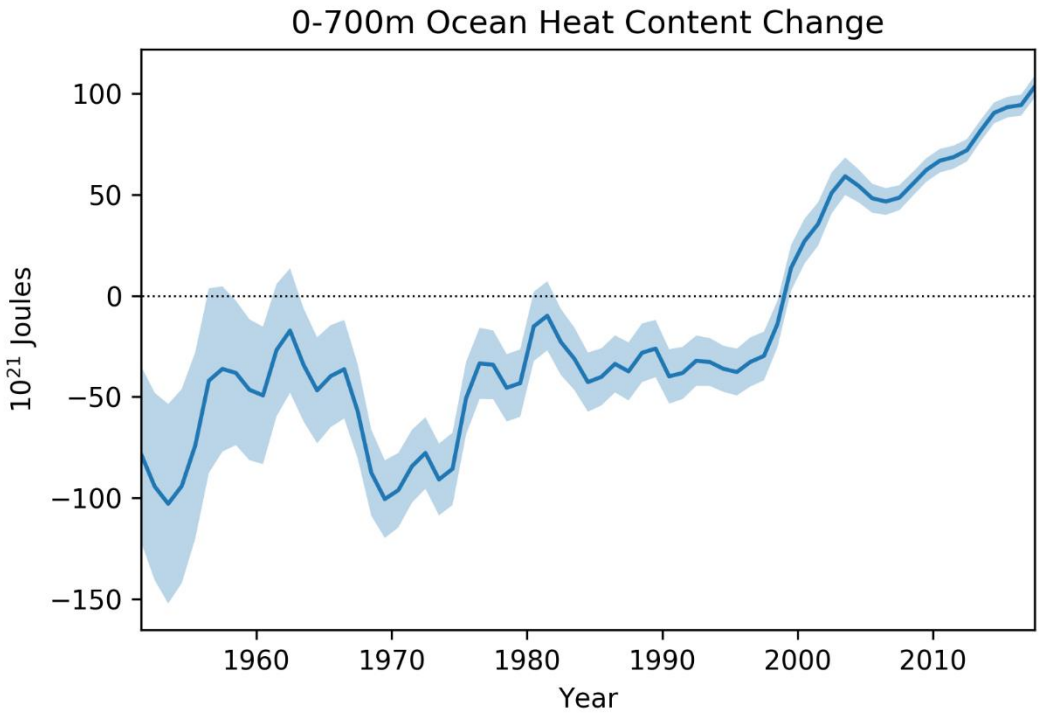

Figure 2: Time series of 0-700m depth global ocean heat content change (10^{21} J) relative to the 1981-2010 average, based on the EN4 quality-controlled subsurface ocean temperature profiles (Good et al, 2013) following Palmer et al. (2007). The shaded regions indicate the 5th to 95th percentiles of uncertainty, following the approach of Palmer and Brohan (2011). Note that uncertainties associated with bias correction and structural uncertainty are not represented. A 1:2:1 smoothing has been applied to the annual data to reduce sampling noise. Source: Good et al. (2013).

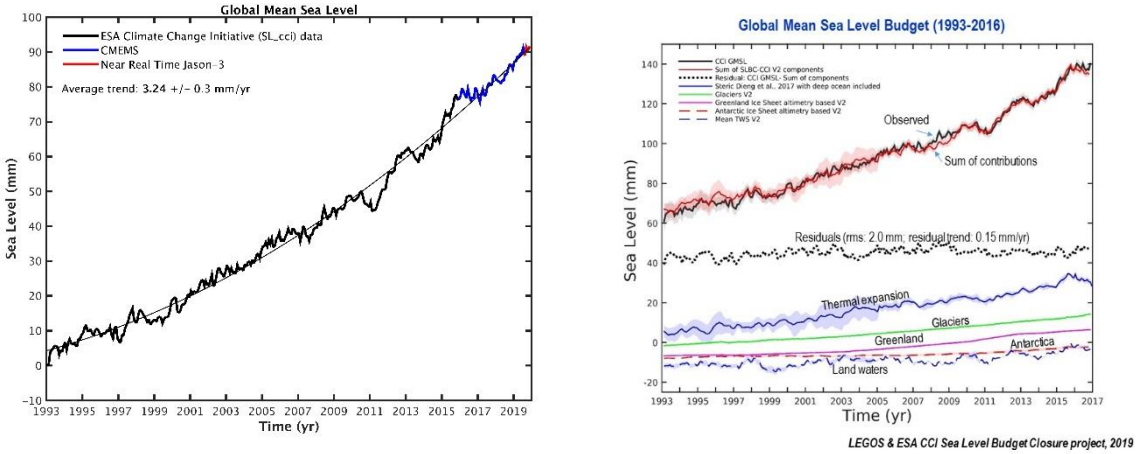

971
972
973 Figure 3. (a) Global mean sea level evolution over January 1993-December 2019 based on
974 multi-mission satellite altimetry. From January 1993 to December 2015, the curve is derived
975 from the ESA Climate Change Initiative sea level product (Legeais et al., 2018). Beyond
976 December 2015, it is extended with sea level data from the Copernicus Marine Environment
977 Monitoring Service (www.marine.copernicus.eu). The last few points of the time series (in
978 red) are based on the near-real time altimetry measurements of the Jason-3 satellite
979 (Source: Laboratoire d'Etudes en Geophysique et Oceanographie Spatiales, EGOS). (b)
980 Global mean sea level budget over 1993-2016. The individual contributions are shown at the
981 bottom of the panel. The altimetry-based sea level and sum of contributions are shown by
982 the black and red curves respectively (Source: ESA Sea level budget Closure project,
983 Horwath et al., 2020).
984

Accepted for publication in *Bulletin of the American Meteorological Society.* DOI 10.1175/BAMS-D-19-0196.1.

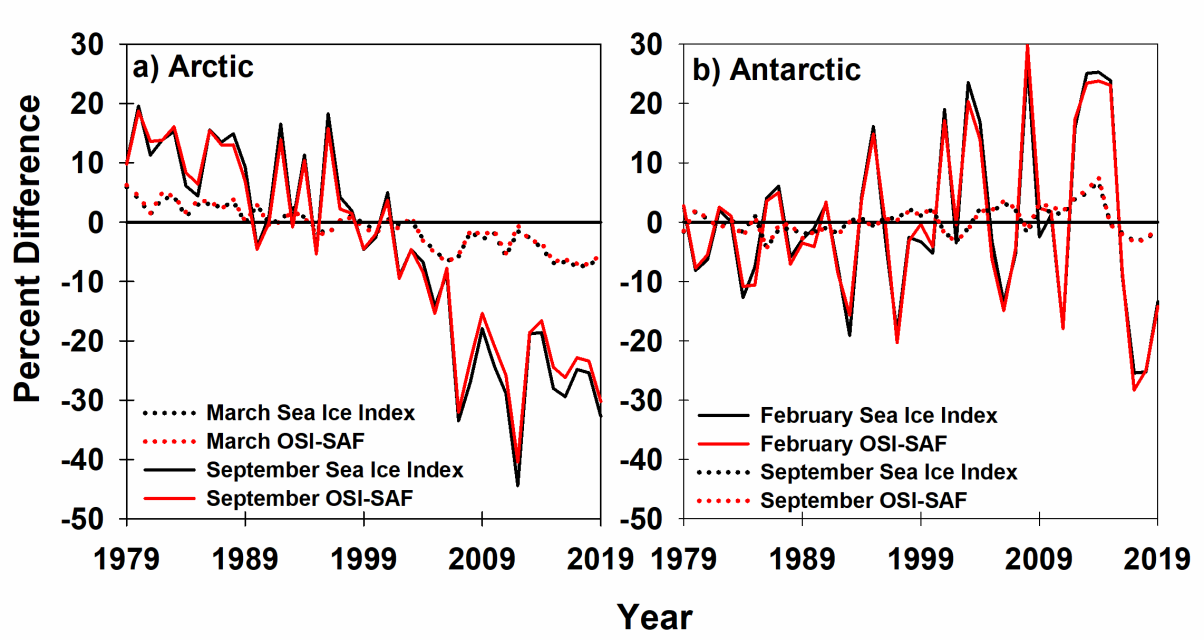

Figure 4. Time series of 1979-2019 sea ice extent anomalies (%) in (a) March (maximum ice extent) and September (minimum ice extent) for the Arctic and (b) in September (maximum ice extent) and February (minimum ice extent) for the Antarctic. The anomaly for each year is the percent difference in sea ice extent relative to the 1981–2010 mean. Sea ice extent is defined as an area covered by sea ice that contains an ice concentration of 15% or greater. Data Source: Sea Ice Index Version 3 (Fetterer et al., 2017) and OSI-SAF Version 2 (Lavergne et al., 2019).

Accepted for publication in *Bulletin of the American Meteorological Society.* DOI 10.1175/BAMS-D-19-0196.1.

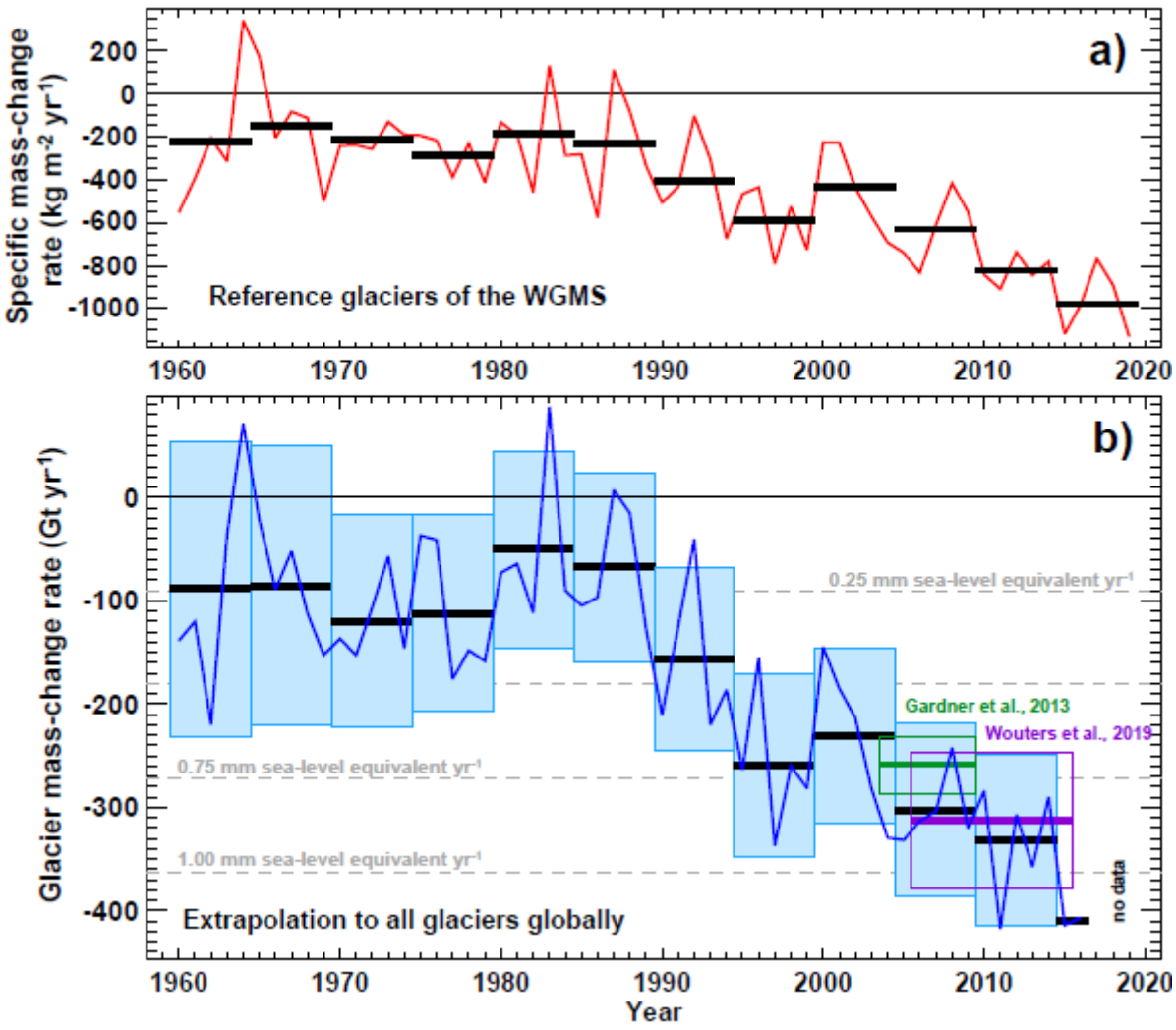

997

998 Figure 5. (a) Average of observed annual specific mass-change rate (red; kg m^{-2} yr^{-1}) of all
999 reference glaciers of the WGMS, including pentadal means (black lines). (b) Annual mass-
1000 change rate (Gt yr^{-1}) of all glaciers outside the two ice sheets (Greenland, Antarctica)
1001 inferred from a combination of remotely sensed glacier thickness changeand annual *in-situ*
1002 observations, according to Zemp et al. (2019). Pentadal averages (black lines) and their
1003 uncertainties (shading) are shown. Global glacier mass-change rates from two independent
1004 studies, primarily based on GRACE results, are shown for comparison (2003-2009 for
1005 Gardner et al., 2013; 2006-2016 for Wouters et al., 2019). Note that results of Wouters et al.
1006 (2019) do not include glaciers in the periphery of Greenland and Antarctica, which have

Accepted for publication in *Bulletin of the American Meteorological Society.* DOI 10.1175/BAMS-D-19-0196.1.

been supplemented for comparability based on Zemp et al. (2019). Source: World Glacier Monitoring Service.

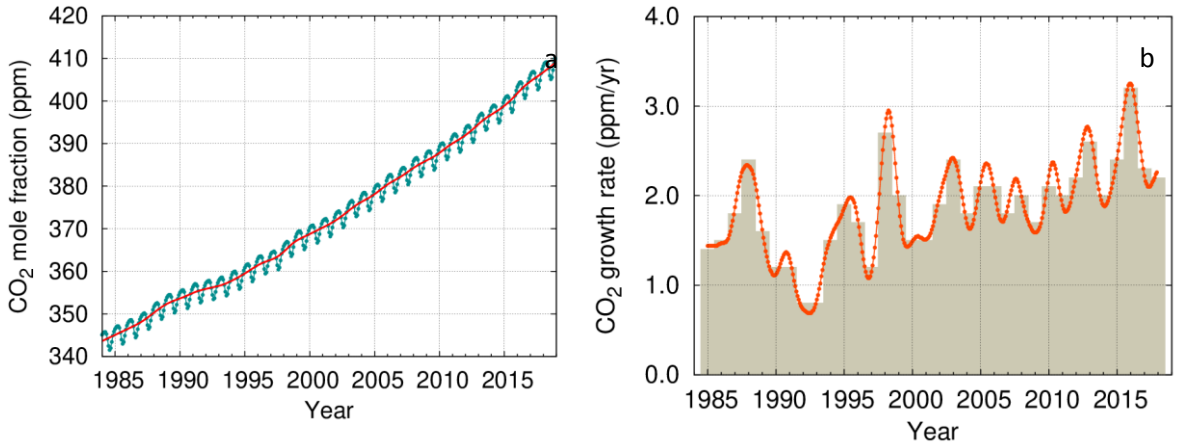

Figure 6. (a) Monthly globally averaged CO_2 mole fraction (ppm) and (b) its growth rate (ppm yr^{-1}) from 1984 to 2018. Increases in successive annual means are shown as the shaded columns in (b). The red line in (a) is the monthly mean with the seasonal variation removed; the blue dots and line depict the raw monthly averages. Source: World Meteorological Organization Greenhouse Gas Bulletin (https://public.wmo.int/en/resources/library/wmo-greenhouse-gas-bulletin).

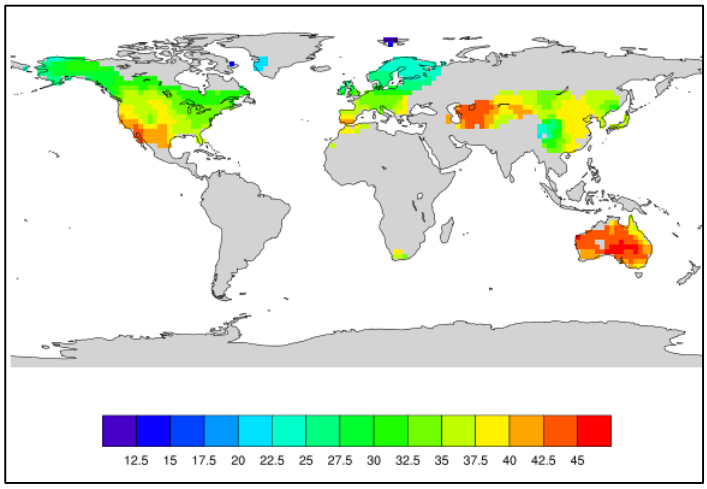

Figure 7. The highest daily maximum temperature (°C) of 2017 from the gridded GHCNDEX extremes indices data set (Donat et al., 2013), illustrating the limited coverage for extremes data in near real time. (Source: University of New South Wales, through www.climdex.org).

Accepted for publication in *Bulletin of the American Meteorological Society.* DOI 10.1175/BAMS-D-19-0196.1.